Bexotegrast Shows Dose-Dependent Integrin $\alpha_v\beta_6$ Receptor Occupancy in Lungs of Participants with Idiopathic Pulmonary Fibrosis: A Phase 2, Open-Label Clinical Trial

Joshua J. Mooney[1], Susan Jacobs[1], Éric A. Lefebvre[3], Gregory P. Cosgrove[3], Annie Clark[3], Scott M. Turner[3*], Martin Decaris[3], Chris N. Barnes[3], Marzena Jurek[3*], Brittney Williams[2], Heying Duan[2], Richard Kimura[2], Gaia Rizzo[4‡], Graham Searle[4‡], Mirwais Wardak[2], and H. Henry Guo[2]

[1]Division of Pulmonary, Allergy and Critical Care, Department of Medicine, and [2]Nuclear Medicine and Molecular Imaging Division, Department of Radiology, Stanford University, Stanford, California; [3]Pliant Therapeutics, Inc., South San Francisco, California; and [4]Invicro, London, United Kingdom

ORCID IDs: 0000-0002-4687-194X (J.J.M.); 0000-0002-8808-0038 (S.J.); 0000-0001-5511-1750 (H.H.G.).

Abstract

Rationale: Idiopathic pulmonary fibrosis (IPF) is a chronic and progressive disease characterized by dyspnea and loss of lung function. Transforming growth factor-β (TGF-β) activation mediated by α_v integrins is central to the pathogenesis of IPF. Bexotegrast (PLN-74809) is an oral, once-daily, dual-selective inhibitor of $\alpha_v\beta_6$ and $\alpha_v\beta_1$ integrins under investigation for the treatment of IPF. Positron emission tomography (PET) using an $\alpha_v\beta_6$-specific PET tracer could confirm target engagement of bexotegrast in the lungs of participants with IPF.

Objectives: This Phase 2 study evaluated $\alpha_v\beta_6$ receptor occupancy in the lung as assessed by changes from baseline in $\alpha_v\beta_6$ PET tracer uptake, after single-dose administration of bexotegrast to participants with IPF.

Methods: In this open-label, single-center study, adults with IPF received up to two single doses of bexotegrast, ranging from 60 to 320 mg with or without background IPF therapy (pirfenidone or nintedanib). At baseline and approximately 4 hours after each orally administered bexotegrast dose, a 60-minute dynamic PET–computed tomography scan was conducted after administration of an $\alpha_v\beta_6$-specific PET probe ([^{18}F]FP-$R_0$1-MG-F2). $\alpha_v\beta_6$ receptor occupancy by bexotegrast was estimated from the changes in PET tracer uptake after bexotegrast administration. Pharmacokinetics, safety, and tolerability of bexotegrast were also assessed.

Results: Eight participants completed the study. Total and unbound plasma bexotegrast concentrations increased in a dose-dependent manner, and regional PET volume of distribution values decreased in a dose- and concentration-dependent manner. The data for volume of distribution fit a simple saturation model, producing an unbound bexotegrast half maximal effective concentration estimate of 3.32 ng/ml. Estimated maximum receptor occupancy was 35%, 53%, 71%, 88%, and 92% after single 60-, 80-, 120-, 240-, and 320-mg doses of bexotegrast, respectively. No treatment-emergent adverse events related to bexotegrast were reported.

Conclusions: Dose and concentration-dependent $\alpha_v\beta_6$ receptor occupancy by bexotegrast was observed by PET imaging, supporting once-daily 160- to 320-mg dosing to evaluate efficacy in clinical trials of IPF.

Clinical trial registered with www.clinicaltrials.gov (NCT 04072315).

Keywords: idiopathic pulmonary fibrosis; PET imaging; receptor occupancy; bexotegrast; integrin $\alpha_v\beta_6$

(Received in original form September 20, 2024; accepted in final form November 5, 2024)

*Former employee of Pliant Therapeutics, Inc.

‡Former employee of Invicro.

Supported by Pliant Therapeutics, Inc., which, as study sponsor, was also involved in the study design, data analysis, and preparation of the manuscript. Editorial assistance was provided by Richard Karpowicz, Ph.D., CMPP, of Nucleus Global, Inc., and was funded by Pliant Therapeutics, Inc.

Ann Am Thorac Soc Vol 22, No 3, pp 350–358, Mar 2025

DOI: 10.1513/AnnalsATS.202409-969OC
Internet address: www.atsjournals.org

Idiopathic pulmonary fibrosis (IPF) is a chronic, progressive form of fibrotic interstitial lung disease of unknown cause (1, 2). IPF is characterized by cough and dyspnea resulting from scarring of the lungs caused by excessive extracellular matrix deposition (1, 3–5). The prognosis of patients with IPF is poor, with a median life expectancy of approximately 3 to 4 years after diagnosis (6, 7).

Transforming growth factor-β (TGF-β) signaling activated by α_v integrins is a key driver of fibrosis in the lungs (8–10). Increased expression of integrins $\alpha_v\beta_6$ on lung epithelial cells and $\alpha_v\beta_1$ on lung fibroblasts activates latent TGF-β (10–13), resulting in SMAD2/3 phosphorylation, profibrotic gene expression, and collagen deposition in the lungs (8, 12, 14). Elevated levels of integrins $\alpha_v\beta_6$ and $\alpha_v\beta_1$ are detectable in the lungs of patients with IPF compared with the lungs of healthy people (12, 15, 16). High levels of integrin $\alpha_v\beta_6$ detected within lung tissue biopsies (17) and elevated integrin subunit β_6 (ITGB6) in plasma (18, 19) are also predictors of worse prognosis for patients with IPF and progressive fibrosing interstitial lung diseases.

TGF-β is involved in multiple different biological functions, and its systemic inhibition can lead to significant safety concerns; as such, there is a need for IPF therapies that inhibit TGF-β signaling specifically at the site of fibrosis (20, 21). Because $\alpha_v\beta_6$ and $\alpha_v\beta_1$ expression levels closely accompany lung injury and fibrogenesis (10, 13), it is proposed that dual-selective inhibition of the $\alpha_v\beta_6/\alpha_v\beta_1$–TGF-β axis may allow for a localized and, therefore, potentially safer approach to reducing TGF-β activation in the fibrotic lung.

Bexotegrast (PLN-74809) is an oral, once-daily, dual-selective inhibitor of $\alpha_v\beta_6$ and $\alpha_v\beta_1$ integrins in development for the treatment of IPF (12). In a Phase 2 study of participants with IPF, bexotegrast showed a favorable safety profile up to 40 weeks of treatment and showed improved lung function and antifibrotic effects based on forced vital capacity (FVC), quantitative lung fibrosis imaging, and circulating levels of plasma ITGB6 and serum type III collagen synthesis neoepitope (22).

An $\alpha_v\beta_6$ cystine knot peptide radiotracer known as the Knottin tracer, [^{18}F]FP-R$_0$1-MG-F2, binds specifically to $\alpha_v\beta_6$ and has been used to detect increased $\alpha_v\beta_6$ expression by positron emission tomography (PET) in the lungs of patients with IPF (15). Noninvasive imaging studies of bexotegrast binding to $\alpha_v\beta_6$ in fibrotic lungs using this tracer could assist in dose selection in future studies, verify access to integrin targets with orally bioavailable agents in the architecturally distorted parenchyma with aberrant pulmonary vasculature in fibrotic lung, and contribute to a comprehensive understanding of receptor occupancy in IPF.

The objective of this Phase 2 study was to evaluate $\alpha_v\beta_6$ receptor occupancy by bexotegrast in the lungs of participants with IPF, as assessed by changes from baseline in $\alpha_v\beta_6$ PET tracer uptake after a single dose of bexotegrast. The safety, tolerability, and pharmacokinetics (PK) of bexotegrast were also explored. Our hypothesis was that bexotegrast and the [^{18}F]FP-R$_0$1-MG-F2 radiotracer bind to the same target in the fibrotic lung and that PET imaging with this radiotracer will noninvasively visualize disease-related receptors and quantify receptor occupancy by bexotegrast in participants with IPF.

A portion of the results of these studies have been previously published in the form of abstracts (23, 24).

Methods

Study Population

This Phase 2 open-label, single-site study (ClinicalTrials.gov ID: NCT 04072315, PLN-74809-IPF-201) was conducted at Stanford University. The study enrolled participants ages 40 years and older with a diagnosis of IPF within 8 years before screening, according to the Fleischner Society White Paper criteria (25), with high-resolution computed tomography (CT) imaging showing a typical or probable usual interstitial pneumonia pattern, FVC percent predicted ⩾45%, and diffusing capacity of the lung for carbon monoxide ($D_{L_{CO}}$) adjusted for hemoglobin values ⩾30%. Background therapy for IPF with pirfenidone or nintedanib was permitted, provided that these drugs had been given at a stable dose for 3 months or more before screening. Key exclusion criteria included receiving any nonapproved agent intended for the treatment of pulmonary fibrosis or IPF, the presence of airway obstruction (ratio <0.7 for forced expiratory volume during 1 second divided by FVC), and known acute IPF exacerbation or suspicion of such within 6 months of screening.

All eligible participants were enrolled in the study and included in the intention to treat (ITT) population. All participants who received at least one dose of bexotegrast were included in the safety population. All participants dosed with a baseline PET scan and at least one postbaseline PET scan were included in the modified ITT (mITT)

Author Contributions: All authors contributed to, reviewed, and approved the final draft of the paper. All authors had full access to all the data in the study and had final responsibility for the decision to submit for publication. Concept and design: J.J.M., É.A.L., G.P.C., S.M.T., and M.D. Development and validation of the positron emission tomography tracer: J.J.M., R.K., and H.H.G. Acquisition, analysis, or interpretation of data: J.J.M., É.A.L., G.P.C., A.C., S.M.T., M.D., C.N.B., H.D., G.R., G.S., and M.W. Drafting of manuscript: all authors. Critical revision of the manuscript for important intellectual content: all authors. Statistical analysis: C.N.B.

Data Sharing Statement: Clinical study data access for research use: Pliant Therapeutics, Inc. ("Pliant") understands and acknowledges the need to share clinical study data with the research community in an open and transparent manner. In furtherance of research efforts, a member of the scientific community may request aggregated deidentified clinical data collected during a clinical study after its public disclosure by Pliant and filing of any related intellectual property protection. To the extent that Pliant has any additional supporting documentation or summary data, it may, at its discretion, also make such information available. Pliant will take into consideration any reasonable request that it receives pertaining to clinical data that has been accepted and published by a journal. Prior to receipt of clinical study data, Pliant and the requesting institution shall enter into an agreement that takes into consideration applicable data privacy laws and the use of the clinical study data for research purposes only. All requests for access to clinical study data must be submitted in writing to scientificcommunications@pliantrx.com.

Correspondence and requests for reprints should be addressed to H. Henry Guo, M.D., Ph.D., Department of Radiology, Stanford University, 435 Quarry Road, Palo Alto, CA 94304. E-mail: henryguo@stanford.edu.

This article has a data supplement, which is accessible at the Supplements tab.

population. The mITT population was used to assess the primary objective of the study. All participants who received at least one dose of bexotegrast and had any measurable bexotegrast concentration data were included in the PK concentration population, and all participants who had sufficient bexotegrast concentration data for PK calculation were included in the PK analysis population.

Study Design

All participants received up to two single oral doses of bexotegrast as a 60-mg oral solution or as an 80-, 120-, 240-, or 320-mg tablet formulation. The planned bexotegrast single doses for this study were selected to approximate steady-state concentrations achieved by daily doses in the Phase 2 INTEGRIS-IPF study (PLN-74809-IPF-202; NCT 04396756) (22).

Participants underwent dynamic PET scans for 60 minutes at baseline (Day −7) and on the day of bexotegrast dosing (Day 1) (Figure 1) after administration of [^{18}F]FP-$R_0$1-MG-F2 for the evaluation of $\alpha_v\beta_6$ receptor occupancy by bexotegrast. Participants were injected with 277.5 MBq (7.5 mCi ± 20%) of [^{18}F]FP-$R_0$1-MG-F2. Postdose imaging for the assessment of $\alpha_v\beta_6$ receptor occupancy was performed to coincide with the anticipated time to maximum observed bexotegrast concentration, approximately 4 hours after administration. PET data were assessed using tracer kinetic models, described in the following text, to determine the total volume of distribution (V_T) in regions of interest (ROIs) within the lung.

After a ⩾14-day washout period, participants could receive a second single bexotegrast dose at a different dose level. If a participant received two single doses, only one baseline predose PET scan was obtained. No more than three PET scans (one at baseline plus one or two post-dosing scans) were obtained for any participant.

This study was conducted in accordance with the study protocol, the Declaration of Helsinki, and the International Council on Harmonisation Good Clinical Practice regulations. The study was approved by the institutional review board of Stanford University. All participants provided written informed consent.

Study Objectives

The primary objective was to evaluate $\alpha_v\beta_6$ receptor occupancy by bexotegrast as assessed by changes from baseline in [^{18}F]FP-$R_0$1-MG-F2 radiotracer uptake in the lung after a single dose of bexotegrast. Secondary objectives included the assessment of safety and tolerability of bexotegrast in participants, as assessed by incidence and severity of treatment-emergent adverse events (TEAEs), as well as clinical safety laboratory measures, vital signs, and electrocardiogram measures. Exploratory endpoints included evaluating the relationship between bexotegrast plasma concentration and PET imaging parameters, changes in V_T from baseline after single doses of bexotegrast, and determination of the unbound plasma concentration of bexotegrast that corresponds to 50% of maximal change (EC_{50}) in V_T.

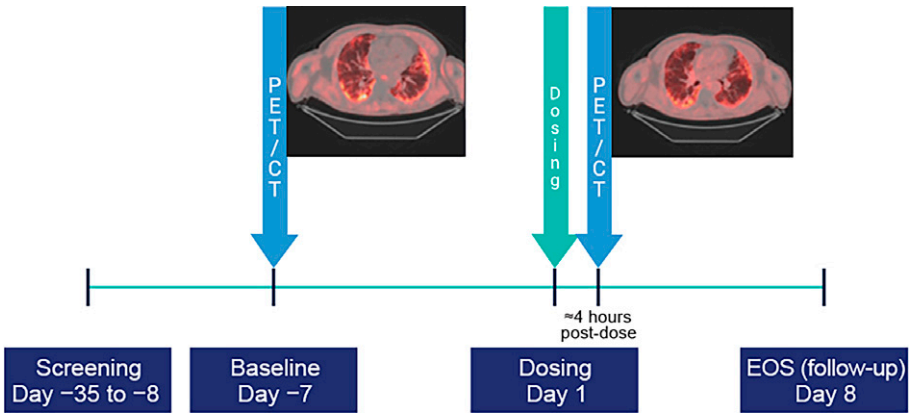

Figure 1. Study design. Participants could elect to receive a second, different dose of bexotegrast after a 14-day washout period. Safety was evaluated through 7 (±2) days after dosing. CT = computed tomography; EOS = end of study; PET = positron emission tomography.

PK Assessments

Bexotegrast plasma PK samples were obtained predose and at 0.5, 1, 2, 3, 4, and 24 hours postdose for determination of total and unbound bexotegrast concentrations. (For details of PK assessments, *see* the Supplemental Methods in the data supplement.)

Image and Data Analysis

PET image processing was performed using Invicro's VivoQuant 2020 software. PET data modeling was performed using Invicro's in-house MIAKAT software package (Version 4.3.25). MIAKAT is implemented using MATLAB R2022a (The Mathworks Inc.).

ROIs selected for image processing included the lungs, cardiac blood pool, and erector spinae muscle. The muscle ROI was defined as the reference region. Blood pool and lung ROIs were used for modeling and analysis. The muscle and cardiac blood pool regions were delineated using fixed spheres with radii of 4 and 5 voxels, respectively, in Invicro's VivoQuant software. Spheres were placed manually using the CT scan for anatomical reference. A semiautomated method using custom MATLAB scripts was used for segmenting the lung ROIs. Preliminary segmentation began by isolating the body in the image from the bed and background. The lungs were then identified as the largest connected component of low attenuation voxels in the body. Morphological open and close operations were used to capture higher attenuation tissue in the lungs. A final quality control, including manual review and editing, was performed to complete the lung segmentations. The segmentation derived from the CT scan was then applied to the PET image to generate time-activity curves (TACs), normalized in standardized uptake value, calculated as radioactivity concentration (kilobecquerels per cubic centimeter)/(radioactivity injected [in megabecquerels] per kilogram of body weight). The top 25th percentile of lung signal at 60 minutes was automatically identified and segmented into a separate ROI (lung25). The lung25 and whole-lung ROIs were used in the modeling and analysis.

Arterial Blood Data Processing

The cardiac blood pool region, defined as the tracer radioactivity in the heart, was used to derive an input function for the kinetic models, assuming no metabolism of the tracer and equal tracer concentration in plasma and whole blood. The blood TAC was smoothed postpeak using a triexponential fit to give the required blood input function.

The resulting blood input function was used as input for the kinetic modeling processes described in the following text.

Kinetic Modeling

The derived tissue TACs were analyzed using the one- and two-tissue compartment models for reversible binding, with fitted blood volume component (26). The aim of the kinetic modeling process was to generate regional estimates of the PET V_T. The most appropriate model was selected as a balance between model parsimony and goodness of fit, assessed through visual inspection of model fits to tissue TACs and parameters such as the Akaike information criterion and the coefficients of variation associated with estimated V_T values. V_T values were calculated for each participant, scan, and ROI.

Signal Change Evaluation

For each participant, the change in tracer uptake after the administration of bexotegrast was calculated from the regional V_T estimates to derive a ΔV_T for each postdose scan (and ROI) as Equation 1:

$$\Delta V_T(\%) = 100\left(\frac{V_{T_{baseline}} - V_{T_{postdose}}}{V_{T_{baseline}}}\right) \quad (1)$$

where $V_{T_{baseline}}$ and $V_{T_{postdose}}$ are the V_T values calculated for the baseline and the postdose scan, respectively. The muscle ROI was included to assess its potential utility as a reference region.

Analysis of the PK-V_T Relationship

The PK-V_T relationship in the study population was explored by plotting the V_T values in lungs against the concentration of unbound bexotegrast in plasma at the time of the PET scan for all scans and participants. These data were fitted with Equation 2:

$$V_T = V_{ND} + V_s\left(1 - \frac{C_p}{C_p + EC_{50}}\right) \quad (2)$$

where V_{ND} is the nondisplaceable volume of distribution, V_S is the specific volume of distribution, C_p is the (measured) unbound concentration in plasma of bexotegrast, and EC_{50} is the plasma concentration of bexotegrast that corresponds to 50% maximal signal change at the time point being studied. Once an estimate of EC_{50} was obtained, estimates of EC_{80} and EC_{90} were calculated using Equation 3:

$$EC_X = EC_{50}\frac{X}{100 - X} \quad (3)$$

where X is the percentage of maximal effect and EC_X is the plasma concentration of

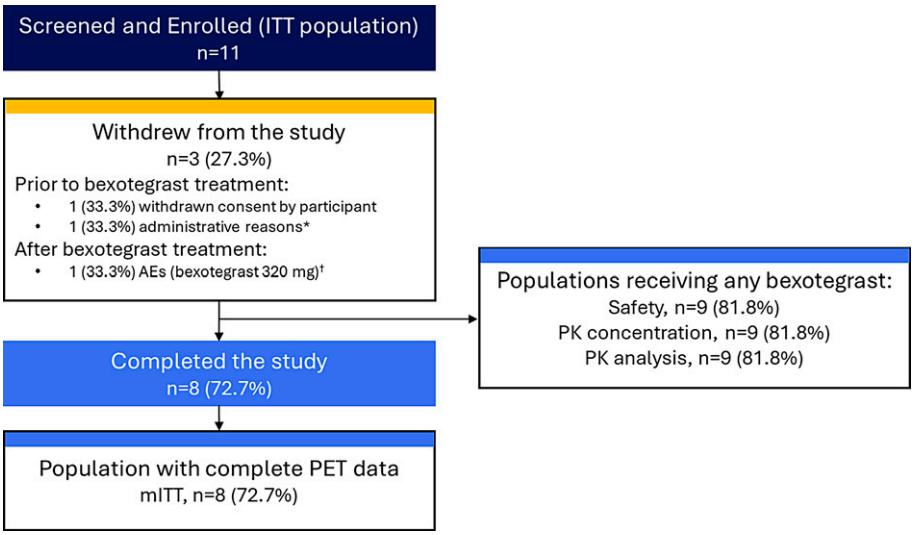

Figure 2. Participant disposition. AE = adverse event; ITT = intention to treat; mITT = modified intention to treat; PET = positron emission tomography; PK = pharmacokinetics.
*Withdrawal was due to sponsor's decision to postpone the study.
†One participant who received 320 mg bexotegrast experienced moderate (Grade 2) treatment-emergent adverse events of hepatic enzyme increased and gamma-glutamyl transferase increased on Day 2 that led to withdrawal from the study on Day 8 and were deemed not related to the study drug. The participant had a medical history of hyperbilirubinemia and was concomitantly receiving nintedanib for treatment of idiopathic pulmonary fibrosis.

Table 1. Baseline demographics and disease characteristics (safety population)

Characteristic	Pooled Bexotegrast (*n* = 9)
Age, yr, mean (SD)	77.6 (4.4)
Sex, *n* (%)	
Male	7 (77.8)
Female	2 (22.2)
Race, *n* (%)	
White	8 (88.9)
Native Hawaiian or other Pacific Islander	1 (11.1)
Weight, kg, mean (SD)	74.6 (13.1)
BMI, kg/m^2, mean (SD)	25.2 (2.47)
FVC, ml, mean (SD)	2,967.8 (829.3)
FVC percent predicted, mean (SD)	83.7 (17.7)
FEV_1, ml, mean (SD)	2,370.0 (554.3)
FEV_1 percent predicted, mean (SD)	98.9 (21.9)
FEV_1/FVC, mean (SD)	0.81 (0.07)
D_{LCO}, mean (SD)	
ml/mmHg/min	13.9 (4.8)
Adjusted percent predicted	63.1 (17.9)
GAP index stage, *n* (%)	
Stage I	5 (55.6)
Stage II	3 (33.3)
Stage III	1 (11.1)
Time since IPF diagnosis, mo, mean (SD)	43.8 (18.5)
Concomitant standard of care treatment, *n* (%)*	
Nintedanib	7 (77.8)
Pirfenidone	1 (11.1)

Definition of abbreviations: BMI = body mass index; D_{LCO} = diffusing capacity for carbon monoxide; FEV_1 = forced expiratory volume in 1 second; FVC = forced vital capacity; GAP = gender–age–physiology; IPF = idiopathic pulmonary fibrosis.
*Concomitant medications are those ongoing at the date and time of first dose of study drug. Participants are counted once within each drug class and once for each unique preferred name.

bexotegrast that corresponds to an effect of X%. For illustrative purposes, a plot of peak effect E (as a percentage of maximal effect) against unbound plasma concentration of bexotegrast was also produced, using Equation 4:

$$E(\%) = 100\frac{C_p}{C_p + EC_{50}} \quad (4)$$

Statistical Analysis

The primary endpoint, change in PET V_T, was summarized using the kinetic modeling as described previously. PK and laboratory data were summarized using standard descriptive statistics. Adverse events data were summarized using the count and proportion of participants.

Results

Study Participants

Participant disposition is reported in Figure 2. A total of 11 participants underwent screening and were enrolled. Eight participants (72.7%) completed the study, and 3 participants (27.3%) withdrew prematurely—2 before bexotegrast dosing (1 each for administrative reasons and withdrawn consent by participant) and 1 after bexotegrast administration.

At baseline, most participants were male, and the mean age was 77.6 years (SD = 4.4) (Table 1). Overall, 7 participants (77.7%) were receiving nintedanib and 1 participant (11.1%) was receiving pirfenidone as background therapy during the study.

PK Assessments

Mean total and unbound plasma bexotegrast concentration–time profiles are presented in Figure 3, indicating dose-dependent increases in plasma bexotegrast concentration. Median time to maximum observed plasma concentration ranged from approximately 2 hours (60 mg) to 3.5 hours (240 mg).

PET Imaging Data

The baseline PET scan and at least one postbaseline PET scan were quantified for 8 study participants (60 mg, $n = 1$; 80 mg, $n = 2$; 120 mg, $n = 3$; 240 mg, $n = 3$; 320 mg, $n = 4$). Images showed heterogenous PET tracer signal in the lung tissue. Example baseline PET, CT, and overlaid PET/CT images demonstrating increased PET tracer uptake in areas of fibrosis are shown elsewhere (*see*

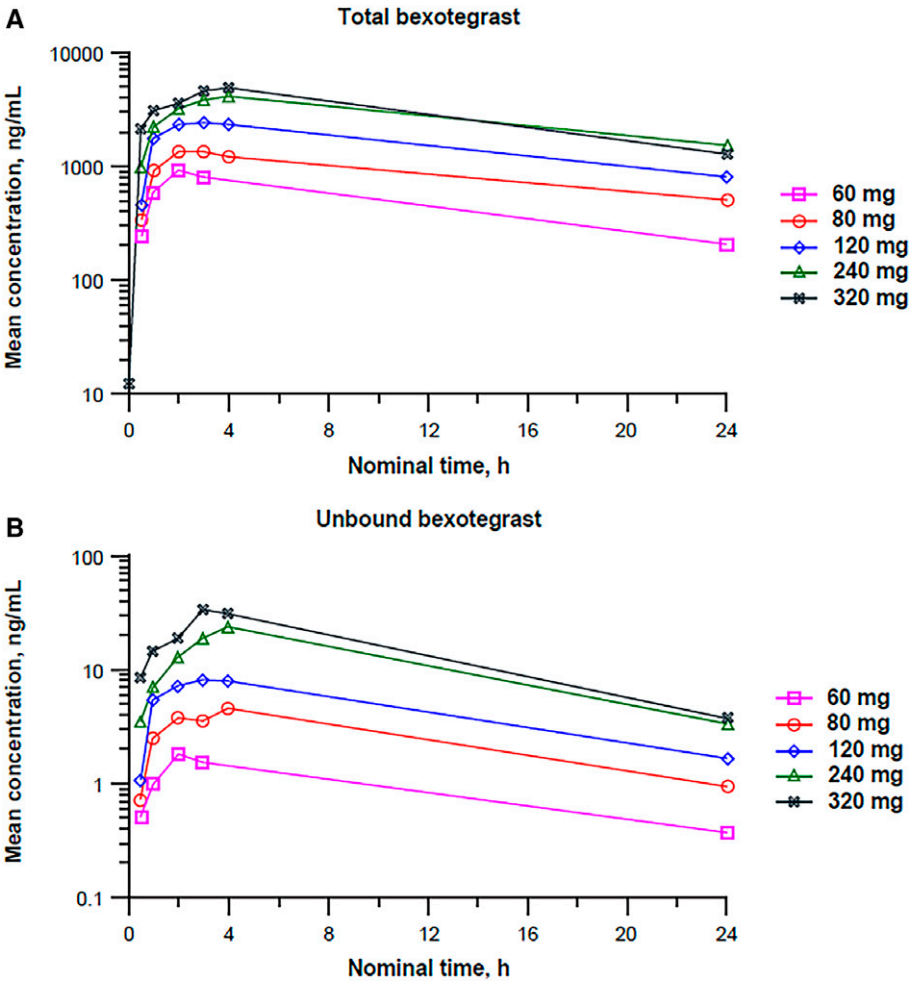

Figure 3. Arithmetic mean (*A*) total and (*B*) unbound plasma bexotegrast concentration versus time profiles after single oral doses of 60 to 320 mg bexotegrast (pharmacokinetic concentration population) (semilogarithmic scale).

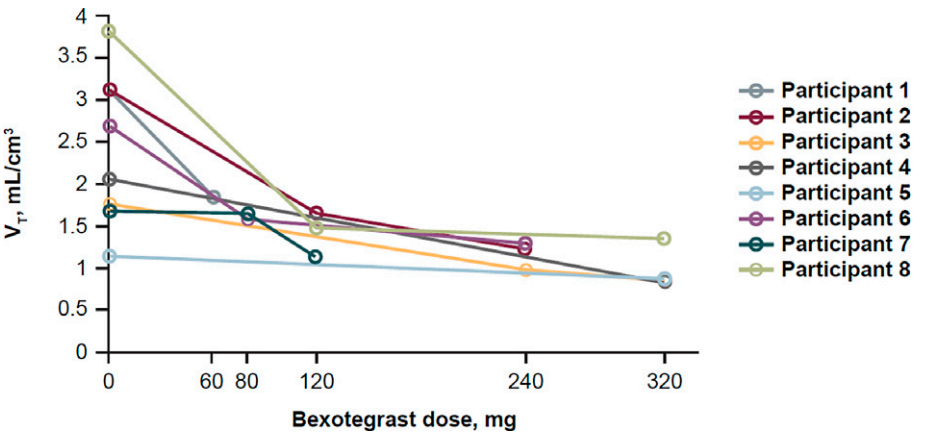

Figure 4. V_T values in the lung25 ROI, plotted against dose of bexotegrast (mITT population). Lung25 = the top 25th percentile of lung signal at 60 minutes; mITT = modified intention to treat; ROI = region of interest; V_T = positron emission tomography volume of distribution.

Figure E1 in the data supplement). Example regional TACs are also shown elsewhere (*see* Figure E2 in the data supplement). In whole lungs and lung25 ROIs, there was typically an early peak within the first few minutes of the tracer injection, representing distribution of the radiolabeled tracer, primarily in the blood volume component of the tissue. This was followed by a period with slower kinetics and markedly higher signal in the lung25 ROI than in the whole lungs, indicating significant heterogeneity within the lungs. Muscle TACs were generally lower and slower than lung TACs.

Kinetic Modeling

Both PET kinetic (one- and two-tissue compartment) models produced visually acceptable model fits to the tissue TACs. As V_T values from both models were similar and highly correlated, the simpler one-tissue compartment model was selected as most appropriate. (For an example of tissue TACs and corresponding one-tissue compartment model fits, *see* Figure E3 in the data supplement.) For baseline scans, the V_T estimates for the lung25 ROI were markedly higher (mean = 2.43 ml/cm^3 [SD = 0.909]; range = 1.14–3.82 ml/cm^3) than for the whole lungs (mean = 1.42 ml/cm^3 [SD = 0.639]; range = 0.57–2.73 ml/cm^3) or muscle (mean = 1.22 ml/cm^3 [SD = 0.500]; range = 0.67–2.00 ml/cm^3).

Signal Change Evaluation upon Bexotegrast Treatment

V_T values generally decreased from baseline after administration of bexotegrast. For all participants, the lung25 ROI showed a dose-dependent decrease in V_T (Figure 4). This decrease was observed in the whole lungs and muscle ROIs as well. Because the V_T values for the muscle ROI consistently decreased from baseline after administration of bexotegrast, its use as a potential reference region was not explored further. Relative decreases in V_T (ΔV_T) were calculated using Equation 1 for lung25, and the magnitude generally increased in a dose-dependent manner (range of ΔV_T: 60 mg bexotegrast, 41.0% [n = 1]; 80 mg, 2.0–41.5%; 120 mg, 33.3–61.4%; 240 mg, 44.6–61.0%; 320 mg, 24.3–64.8%).

Analysis of the PK-V_T Relationship

PET scans were commenced approximately 4 hours after administration of bexotegrast. PK data were available for the nominal 4-hour time point for 12 of the 13 postdose scans. The 3-hour time point was used in place of the missing 4-hour time point for 1 scan.

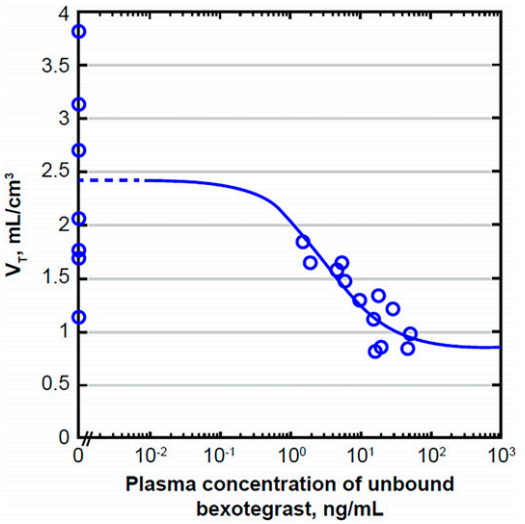

Figure 5. Plot of V_T in the lung25 ROI against unbound plasma concentration of bexotegrast, together with a model fit using Equation 2 (mITT population). Lung25 = the top 25th percentile of lung signal at 60 minutes; mITT = modified intention to treat; ROI = region of interest; V_T = positron emission tomography volume of distribution.

V_T values for the lung25 ROI are plotted against unbound plasma concentration values in Figure 5. Model fit parameters that were estimated by fitting Equation 2 to the PK and V_T data together are shown in Table 2. The estimated EC_{50} for the lung25 ROI was 3.32 ng/ml (95% confidence interval, −4.19 to 10.83), corresponding, through Equation 3, to an EC_{80} of approximately 13.3 ng/ml and an EC_{90} of approximately 29.9 ng/ml.

Receptor occupancy of $\alpha_v\beta_6$ by bexotegrast, suggested by treatment-induced changes in V_T, was observed to be dose and concentration dependent, with estimated mean (range) maximum receptor occupancy of 35% (n = 1), 53% (37–63%), 71% (62–83%), 88% (64–94%), and 92% (83–96%) after administration of single doses of 60, 80, 120, 240, and 320 mg bexotegrast, respectively (Figure 6). Representative PET images at baseline and after administration of bexotegrast 320 mg are shown in Figure 7. Bexotegrast doses of ⩾80 mg resulted in peak mean unbound concentrations above the estimated EC_{50} (*see* Table E1 in the data supplement).

Safety

No serious TEAEs were reported, and no participant experienced a TEAE that was related to study drug (*see* Table E2 in the data supplement). One participant (who received a single dose of 320 mg bexotegrast) experienced TEAEs on treatment. These were moderate (Grade 2) TEAEs of hepatic enzyme increased and gamma-glutamyl transferase increased on Day 2 that led to withdrawal from the study on Day 8 and were deemed not related to the study drug.

Table 2. Model fit parameters estimated by fitting Equation 2 to the PK and V_T data (mITT population)

	Fitted Model Parameters		
ROI	**EC_{50} (ng/ml)**	**V_{ND} (ml/cm^3)**	**V_S (ml/cm^3)**
Lung25	3.32	0.86	1.56
Whole lungs	3.36	0.54	0.87

Definition of abbreviations: EC_{50} = half maximal effective concentration; lung25 = the top 25th percentile of lung signal at 60 minutes; mITT = modified intention to treat; PK = pharmacokinetic; ROI = region of interest; V_{ND} = nondisplaceable volume of distribution; V_S = specific volume of distribution; V_T = positron emission tomography volume of distribution.

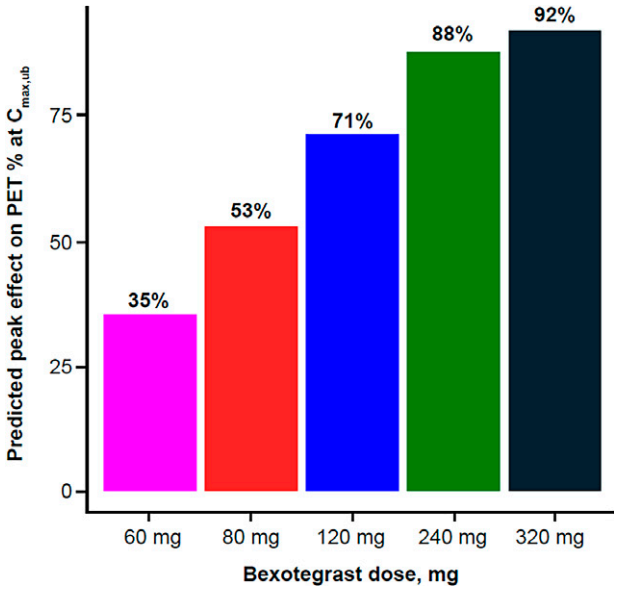

Figure 6. Predicted peak effect after single doses of bexotegrast, based on the mean unbound C_{max} data and the model of Equation 4* (mITT population). C_{max} = maximum observed concentration; mITT = modified intention to treat; PET = positron emission tomography; ub = unbound bexotegrast.
*Bexotegrast pharmacokinetic data from all participants enrolled in the study were used to estimate the mean C_{max}.

The participant had a medical history of hyperbilirubinemia, which was considered an alternative causality. This participant was concomitantly receiving nintedanib for treatment of IPF, with known adverse reactions of liver enzyme elevations (27), and nintedanib dosing was stopped on Day 8. Hematology, clinical chemistry, urinalysis, physical examination findings, and vital sign parameters remained stable over time, and there were no clinically significant echocardiogram changes during the treatment period. No deaths occurred during the study.

Discussion

There exists an unmet medical need for a safe treatment that is capable of inhibiting and potentially reversing fibrosis in the lungs of patients with IPF. Currently available IPF therapies, nintedanib and pirfenidone, reduce the decline of lung function and potentially improve survival with continuous treatment (28–32). However, these drugs do not inhibit the progression of IPF, and they do not consistently improve patients' quality of life (30, 32). The tolerability of these two agents also remains a challenge, resulting in some patients with IPF having to discontinue treatment or undergo dose reductions (33).

Although TGF-β signaling is an attractive target for IPF drug development, safety concerns associated with systemic TGF-β inhibition highlight the need for specificity within fibrotic tissue. Localized TGF-β inhibition in the fibrotic lung, achieved by inhibiting $\alpha_v\beta_6$ and $\alpha_v\beta_1$ integrins with bexotegrast, may provide a novel approach for treating IPF without affecting TGF-β signaling systemically.

In the present study, we investigated the dose and exposure response of bexotegrast with $\alpha_v\beta_6$ integrin by performing PET imaging with a competitive $\alpha_v\beta_6$-binding probe, [^{18}F]FP-$R_0$1-MG-F2 (15), at or near the maximum observed concentration of bexotegrast (a plain-language infographic is provided elsewhere; *see* the data supplement PDF titled "PLS_Infographic"). V_T values in the lung25 and whole-lung ROIs decreased in a dose- and concentration-dependent manner, consistent with bexotegrast binding to $\alpha_v\beta_6$ integrin in the lungs, suggesting that doses between 120 mg and 320 mg may provide optimal receptor occupancy and providing further support for the 160-mg and 320-mg doses currently evaluated in the ongoing Phase 2b/3 BEACON-IPF study (ClinicalTrials.gov ID: NCT 06097260, PLN-74809-IPF-206). No corrections for air volume fraction were made, so the signal in lungs per unit volume of solid tissue may be more elevated relative to other tissues than the V_T values suggest. These results support receptor occupancy of bexotegrast to $\alpha_v\beta_6$ integrin present in fibrotic tissue in the lungs of participants with IPF. Although not directly assessed in the present study, we anticipate a similar rate of receptor occupancy for $\alpha_v\beta_1$ integrins, given that the IC_{50} of bexotegrast

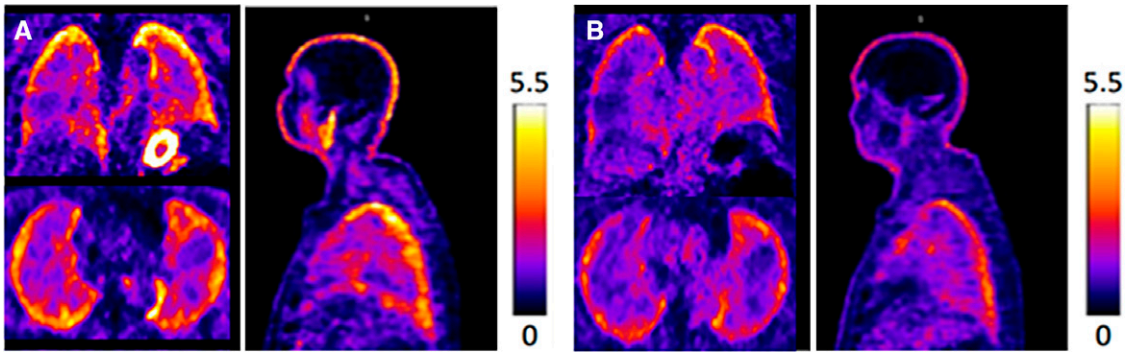

Figure 7. Knottin positron emission tomography (PET) images of the lungs in coronal, axial, and sagittal projections at baseline (*A*) and posttreatment with a 320-mg dose of bexotegrast (*B*) demonstrating decreased tracer uptake by lungs after drug treatment, consistent with integrin $\alpha_v\beta_6$ binding by bexotegrast and competitive inhibition of knottin tracer binding posttreatment.

is roughly equipotent for $\alpha_v\beta_1$ and $\alpha_v\beta_6$ integrins in both ligand binding and TGF-β activation assays (12). Bexotegrast was well tolerated at the doses administered in the present study, with no participants experiencing serious TEAEs or TEAEs related to bexotegrast treatment.

In a previous Phase 1 study in participants with IPF that included PET imaging with an $\alpha_v\beta_6$-specific PET ligand [^{18}F]FB-A20FMDV2, $\alpha_v\beta_6$ receptor occupancy by the integrin inhibitor GSK3008348 was observed (34). A strength of both the GSK3008348 study and the current PET study is the ability to observe receptor occupancy directly in the affected fibrotic lung tissue of participants with IPF, in contrast to other assay systems such as those using peripheral blood mononuclear cells. Although PET has not been widely used to demonstrate receptor occupancy in IPF, both studies support the further use of PET in IPF drug development.

Bexotegrast was also evaluated in the global Phase 2 INTEGRIS-IPF study (ClinicalTrials.gov ID: NCT 04396756, PLN-74809-IPF-202) (22). Participants with IPF who received 40, 80, 160, or 320 mg bexotegrast for up to 12 weeks experienced a favorable safety and tolerability profile, with no dose relationship for TEAEs observed. Dose-proportional increases in bexotegrast plasma concentrations were observed, which were consistent with the present PET results. Analyses in INTEGRIS-IPF—including FVC, quantitative lung fibrosis scores, and circulating levels of fibrosis and IPF progression biomarkers—suggested an antifibrotic effect of bexotegrast treatment.

Limitations of this study include the relatively small sample size of the study, with only 8 participants completing PET imaging after bexotegrast treatment. Although the study population had a mean age of 77.6 years with relatively well-preserved FVC and $D_{L_{CO}}$, the $\alpha_v\beta_6$ integrin binding observed here is expected to be generalizable across younger patients and those with worse disease severity. Given the slow kinetics of the [^{18}F]FP-$R_0$1-MG-F2 radiotracer, a longer acquisition time may have been informative and enabled an evaluation of optimal scan duration; however, longer acquisition times may be uncomfortable for participants with IPF. Test–retest studies are needed to confirm the sensitivity of this method for estimating $\alpha_v\beta_6$ receptor occupancy.

In summary, after a single dose of bexotegrast, dose– and concentration-dependent $\alpha_v\beta_6$ integrin receptor occupancy was observed by means of PET over the 60- to 320-mg dose range. This effect is consistent with the hypothesis that bexotegrast engages with $\alpha_v\beta_6$ integrin receptors in the lungs. Bexotegrast was well tolerated at the administered doses, with no bexotegrast-related TEAEs or serious TEAEs reported during this study. Overall, this study supports the late-stage evaluation of bexotegrast at 160-mg and 320-mg doses in the ongoing Phase 2b/3 BEACON-IPF trial (ClinicalTrials.gov ID: NCT 06097260) in IPF. ■

Author disclosures are available with the text of this article at www.atsjournals.org.

Acknowledgment: The authors thank the patients who volunteered to participate in this study (ClinicalTrials.gov ID: NCT04072315; PLN-74809-201). The authors also thank Michael Maker, who was an employee of Invicro at the time of this study, for his assistance with the data analysis and Karen Morris, Ph.D., the Stanford University research coordinator, for the successful recruitment and enrollment efforts for this study.

References

1 Lederer DJ, Martinez FJ. Idiopathic pulmonary fibrosis. *N Engl J Med* 2018;378:1811–1823.
2 Raghu G, Collard HR, Egan JJ, Martinez FJ, Behr J, Brown KK, *et al.*; ATS/ERS/JRS/ALAT Committee on Idiopathic Pulmonary Fibrosis. An official ATS/ERS/JRS/ALAT statement: idiopathic pulmonary fibrosis: evidence-based guidelines for diagnosis and management. *Am J Respir Crit Care Med* 2011;183:788–824.
3 Maher TM, Bendstrup E, Dron L, Langley J, Smith G, Khalid JM, *et al.* Global incidence and prevalence of idiopathic pulmonary fibrosis. *Respir Res* 2021;22:197.
4 Booth AJ, Hadley R, Cornett AM, Dreffs AA, Matthes SA, Tsui JL, *et al.* Acellular normal and fibrotic human lung matrices as a culture system for *in vitro* investigation. *Am J Respir Crit Care Med* 2012;186:866–876.
5 Guo H, Sun J, Zhang S, Nie Y, Zhou S, Zeng Y. Progress in understanding and treating idiopathic pulmonary fibrosis: recent insights and emerging therapies. *Front Pharmacol* 2023;14:1205948.
6 Raghu G, Chen SY, Yeh WS, Maroni B, Li Q, Lee YC, *et al.* Idiopathic pulmonary fibrosis in US Medicare beneficiaries aged 65 years and older: incidence, prevalence, and survival, 2001–11. *Lancet Respir Med* 2014;2:566–572.
7 Strongman H, Kausar I, Maher TM. Incidence, prevalence, and survival of patients with idiopathic pulmonary fibrosis in the UK. *Adv Ther* 2018;35: 724–736.
8 Saito A, Horie M, Nagase T. TGF-β signaling in lung health and disease. *Int J Mol Sci* 2018;19:2460.
9 Henderson NC, Sheppard D. Integrin-mediated regulation of TGFβ in fibrosis. *Biochim Biophys Acta* 2013;1832:891–896.
10 Reed NI, Jo H, Chen C, Tsujino K, Arnold TD, DeGrado WF, *et al.* The $\alpha_v\beta_1$ integrin plays a critical in vivo role in tissue fibrosis. *Sci Transl Med* 2015;7:288ra79.
11 Robertson IB, Rifkin DB. Regulation of the bioavailability of TGF-β and TGF-β-related proteins. *Cold Spring Harb Perspect Biol* 2016;8:a021907.
12 Decaris ML, Schaub JR, Chen C, Cha J, Lee GG, Rexhepaj M, *et al.* Dual inhibition of $\alpha_v\beta_6$ and $\alpha_v\beta_1$ reduces fibrogenesis in lung tissue explants from patients with IPF. *Respir Res* 2021;22:265.
13 Munger JS, Huang X, Kawakatsu H, Griffiths MJ, Dalton SL, Wu J, *et al.* The integrin αvβ6 binds and activates latent TGF β1: a mechanism for regulating pulmonary inflammation and fibrosis. *Cell* 1999;96:319–328.
14 Flanders KC. Smad3 as a mediator of the fibrotic response. *Int J Exp Pathol* 2004;85:47–64.
15 Kimura RH, Wang L, Shen B, Huo L, Tummers W, Filipp FV, *et al.* Evaluation of integrin $\alpha v\beta_6$ cystine knot PET tracers to detect cancer and idiopathic pulmonary fibrosis. *Nat Commun* 2019;10:4673.
16 Horan GS, Wood S, Ona V, Li DJ, Lukashev ME, Weinreb PH, *et al.* Partial inhibition of integrin αvβ6 prevents pulmonary fibrosis without exacerbating inflammation. *Am J Respir Crit Care Med* 2008;177:56–65.
17 Saini G, Porte J, Weinreb PH, Violette SM, Wallace WA, McKeever TM, *et al.* αvβ6 integrin may be a potential prognostic biomarker in interstitial lung disease. *Eur Respir J* 2015;46:486–494.
18 Bowman WS, Newton CA, Linderholm AL, Neely ML, Pugashetti JV, Kaul B, *et al.* Proteomic biomarkers of progressive fibrosing interstitial lung disease: a multicentre cohort analysis. *Lancet Respir Med* 2022; 10:593–602.
19 Oldham JM, Huang Y, Bose S, Ma SF, Kim JS, Schwab A, *et al.* Proteomic biomarkers of survival in idiopathic pulmonary fibrosis. *Am J Respir Crit Care Med* 2024;209:1111–1120.
20 Shi N, Wang Z, Zhu H, Liu W, Zhao M, Jiang X, *et al.* Research progress on drugs targeting the TGF-β signaling pathway in fibrotic diseases. *Immunol Res* 2022;70:276–288.
21 Maher JM, Zhang R, Palanisamy G, Perkins K, Liu L, Brassil P, *et al.* Lung-restricted ALK5 inhibition avoids systemic toxicities associated with TGFβ pathway inhibition. *Toxicol Appl Pharmacol* 2022;438: 115905.

22 Lancaster L, Cottin V, Ramaswamy M, Wuyts WA, Jenkins RG, Scholand MB, *et al.*; PLN-74809-IPF-202 Trial Investigators. Bexotegrast in patients with idiopathic pulmonary fibrosis: the INTEGRIS-IPF Study. *Am J Respir Crit Care Med* 2024;210:424–434.
23 Mooney JJ, Morris K, Jacobs S, Lefebvre E, Cosgrove GP, Wong S, *et al.* PLN-74809, a dual-selective inhibitor of integrins αvβ6 and αvβ1, shows dose-dependent target engagement in the lungs of patients with idiopathic pulmonary fibrosis (IPF) [abstract]. *Am J Respir Crit Care Med* 2022;205:A5254.
24 Wardak M, Turner S, Mooney J, Rizzo G, Morris K, Su J, *et al.* Phase 2 drug target engagement study of PLN-74809 in patients with idiopathic pulmonary fibrosis using a novel αvβ6 cystine knot PET imaging tracer. *J Nucl Med* 2022;63:2236.
25 Lynch DA, Sverzellati N, Travis WD, Brown KK, Colby TV, Galvin JR, *et al.* Diagnostic criteria for idiopathic pulmonary fibrosis: a Fleischner Society white paper. *Lancet Respir Med* 2018;6:138–153.
26 Gunn RN, Slifstein M, Searle GE, Price JC. Quantitative imaging of protein targets in the human brain with PET. *Phys Med Biol* 2015;60: R363–R411.
27 Ofev (nintedanib capsules) [prescribing information]. Ridgefield, CT: Boehringer Ingelheim Pharmaceuticals, Inc., 2024. Available from: https://content.boehringer-ingelheim.com/DAM/b5d67da8-329b-4fa4-a732-af1e011fc0a5/ofev-us-pi.pdf.
28 Lancaster L, Crestani B, Hernandez P, Inoue Y, Wachtlin D, Loaiza L, *et al.* Safety and survival data in patients with idiopathic pulmonary fibrosis treated with nintedanib: pooled data from six clinical trials. *BMJ Open Respir Res* 2019;6:e000397.
29 Nathan SD, Albera C, Bradford WZ, Costabel U, Glaspole I, Glassberg MK, *et al.* Effect of pirfenidone on mortality: pooled analyses and meta-analyses of clinical trials in idiopathic pulmonary fibrosis. *Lancet Respir Med* 2017;5:33–41.
30 King TE, Bradford WZ, Castro-Bernardini S, Fagan EA, Glaspole I, Glassberg MK, *et al.*; ASCEND Study Group. A phase 3 trial of pirfenidone in patients with idiopathic pulmonary fibrosis. *N Engl J Med* 2014;370:2083–2092.
31 Petnak T, Lertjitbanjong P, Thongprayoon C, Moua T. Impact of antifibrotic therapy on mortality and acute exacerbation in idiopathic pulmonary fibrosis: a systematic review and meta-analysis. *Chest* 2021;160:1751–1763.
32 Richeldi L, Du Bois RM, Raghu G, Azuma A, Brown KK, Costabel U, *et al.*; INPULSIS Trial Investigators. Efficacy and safety of nintedanib in idiopathic pulmonary fibrosis. *N Engl J Med* 2014;370:2071–2082.
33 Levra S, Guida G, Sprio AE, Crosa F, Ghio PC, Bertolini F, *et al.* Long-term safety of antifibrotic drugs in IPF: a real-world experience. *Biomedicines* 2022;10:3229.
34 Maher TM, Simpson JK, Porter JC, Wilson FJ, Chan R, Eames R, *et al.* A positron emission tomography imaging study to confirm target engagement in the lungs of patients with idiopathic pulmonary fibrosis following a single dose of a novel inhaled αvβ6 integrin inhibitor. *Respir Res* 2020;21:75.